Tuning of the silicon nitride refractive index by RF sputtering power

Daniela De Luca[a,b,*], Emiliano Di Gennaro[a,b], Davide De Maio[b,c], Carmine D'Alessandro[b,c], Antonio Caldarelli[b,c], Marilena Musto[b,c], Can Koral[d], Antonello Andreone[a,d,e], Valentina Di Meo[b], Mario Iodice[b], Roberto Russo[b]

[a] *Department of Physics, University of Naples "Federico II", 80126 Napoli, Italy*
[b] *Consiglio Nazionale delle Ricerche, Istituto di Scienze Applicate e Sistemi Intelligenti, 80131 Napoli, Italy*
[c] *Department of Industrial Engineering, University of Napoli "Federico II", Napoli, Italy.*
[d] *National Institute for Nuclear Physics, UdR Napoli,80126 Napoli, Italy*
[e] *CNR-SPIN, UOS Napoli, via Cinthia, 80126 Napoli, Italy.*

Abstract

The fabrication of thin-film multilayer structures by sputtering technique usually requires multi-cathode deposition machine. This study proposes a simpler approach based on the RF power modulation: silicon nitride (SiN_x) thin films were prepared by RF reactive sputtering in (Ar + N_2) atmosphere at room temperature. The samples were analyzed to highlight the effects of different deposition conditions on the morphological and optical properties of the films in the visible and near/mid-IR regions. The refractive index of the films was changed in the range of 1.5 - 2.5 (at λ=800 nm) by tuning the sputtering power. IR reflectance measurements revealed the absence of spurious (oxygen- or hydrogen-based) phases, while atomic force and scanning electron microscopies confirmed the presence of flat and defect-free samples surfaces.

Keywords: Silicon nitride, RF sputtering, refractive index, FTIR, AFM, SEM

1. Introduction

Silicon nitride exhibits optical, thermal, mechanical, and electric properties [1] that make it desirable and successful in many research sectors and industrial applications since the '80s: it has been employed in the field of semiconductors [2], metallurgy [3], microelectronics and integrated circuits [4], optics [5], and solar cells [6]. The silicon nitride films can be deposited by different methods; in the past they have been usually prepared by chemical vapor deposition (CVD) techniques, causing those hydrogen-rich coatings to undergo degradation when subject to high temperature treatments [7]. Currently, sputtering depositions are preferred since they allow to obtain films with low hydrogen contents, and with easily customizable properties and stoichiometry [8].

So far, several works have been already conducted on silicon nitride, demonstrating that its physical properties are strongly influenced by the substrate temperature [9] and N_2 partial pressure [10]. In particular, the influence of the Ar and N_2 gases concentration on the refractive index and deposition rate of silicon nitride films have been studied, showing that the increase in nitrogen flux leads to higher refractive indices and lower deposition rates [11, 12].

By converse, in the present study, numerous silicon nitride films have been prepared at room temperature by using a Si cathode in an RF magnetron sputtering apparatus, keeping the Ar and N_2 gases concentrations fixed while varying the sputtering power. This aims at the production of samples with manageable properties, and intends to broaden the knowledge of the silicon nitride properties by looking at both its morphology and its optical properties. It includes various novelties, ranging from the study of the influence of RF power on deposition rates and refractive index dispersion curves in the range of 300 to 1600 nm, to the analysis

*Corresponding author: daniela.deluca@unina.it; daniela.deluca@na.isasi.cnr.it

of the reflectance spectra both in the VIS and in the near/mid-IR regions, where Si-N chemical bonds have been highlighted. Atomic Force Microscopy (AFM) and Scanning Electron Microscopy (SEM) shown flat and defect-free sample surfaces. In addition, the reproducibility of the deposition process has also been verified, proving the feasibility of multilayers easy to be fabricated and to be used in applications involving complex structures like rugate filters, Bragg mirrors, or the Gradient-index (GRIN) optics technology.

2. Experimental Details

2.1. Samples production

Silicon nitride thin films were produced by reactive sputtering depositions, by using a magnetron source operated by an RF power supply. A water cooled silicon target (4-inch diameter) with purity of 99.99% has been placed at a fixed distance from the samples holder. Smooth glasses (Corning: 1737F) were used as substrates, after an appropriate cleaning in acetone and isopropanol baths in an ultrasonic washing. To facilitate optical studies also lightly n-type doped (1.0 - $1.5 \cdot 10^{-3}\,\Omega \cdot$ cm) single-side polished silicon (100) wafers have been used as substrates.
The vacuum chamber is pumped down to a base pressure of 10^{-5} Pa. High-purity Ar and N_2 gases were introduced into the chamber and monitored by two separate mass flow controllers (MKS, Series 946), with a constant Ar to N_2 ratio (36:3) corresponding to a partial pressure of 0.54 Pa. The choice of fixing the argon flow to be highly larger than that of nitrogen is based on evidence from previous works [13, 14], where it is demonstrated that increasing the total pressure of the processing gas could reduce the hysteresis that characterizes most of the reactive sputtering processes. Before starting the depositions, the Si target is pre-sputtered by slowly increasing the RF power and keeping it at the desired value for 20 minutes. This ensures the achievement of an equilibrium condition and guarantees a homogeneous film growth. This conditioning is performed with the shutter plate open and using an empty sample holder to reproduce the same conditions of an actual experiment. In this experiment, the silicon target has been supplied with different powers, in the range of $100\,W$ to $400\,W$. No external heating was provided during the depositions.

2.2. Samples characterization

Film thickness was measured by means of a profilometer (KLA Tencor, P-15) after effecting a lift-off procedure on the samples soaked in acetone. The result was then compared and confirmed by ellipsometric analysis. The deposition rate was calculated by the ratio of the measured thickness by the deposition time. The refractive index of each film was investigated by means of a spectroscopic ellipsometer (Horiba Jobin-Yvon, UVISEL) equipped with a xenon lamp and a detector system for the analysis of the sample optical response in a range between 280 and 1600 nm. Ellipsometric measurements are based on the collection of the change in polarization as the incident radiation interacts with the material structure of interest; the polarization change is quantified by the amplitude ratio and the phase difference. The measured response depends on optical properties and thickness of individual materials. The measured data are used to validate a material structure model that, by means of mathematical relations (*dispersion formulae*), returns the material optical properties. In our case, the complex refractive index of silicon nitride film was well fitted by the Tauc-Lorentz dispersion formula [15, 16].

Reflectivity measurements of each sample have been performed in the spectral range of 350 nm to 1750 nm, by using an integrating sphere (Ocean Optics ISP-REF) coupled with an Optical Spectrum Analyser (OSA) by means of an optical fiber. Each measurement is then normalized using a calibrated reflectance standard, WS-1_SL. The optical response of the produced samples has been further investigated by a Fourier Transform InfraRed (FTIR) spectrometer, in the range of $1.4\,\mu m$ to $10\,\mu m$ (Jasco FT/IR 6300). Both measurements have been compared with results from simulations performed with the software *Open Filters* (OF) [17]. Morphological analysis by Atomic Force Microscopy (AFM) and Scanning Electron Microscope (SEM) measurements have also been carried out.

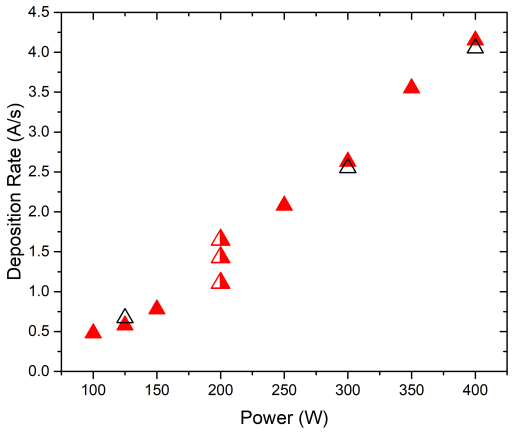

Figure 1: Deposition rate of silicon nitride at various RF sputtering powers (red triangles). Black empty triangles represent additional samples produced to check the rates reproducibility, while the red half empty ones highlight the lack of reproducibility in the region around 200 W.

3. Results and Discussions

3.1. Deposition rate and refractive index

During the reactive sputtering, the gases react with the material of the target creating a compound which condensate on the substrate. The speed of this phenomenon, as well as the properties of the compound, is process-dependent. It has been found that, at a fixed Ar and N_2 pressures, the deposition rate increases linearly with the sputtering power, as shown in Fig. 1, according with results of prior works conducted over narrower range of powers [18, 19]. The figure also shows a good stability of the deposition rate over the whole range of investigated powers, except for the region around 200 W, where the lack of reproducibility in the deposition rate also corresponds to a lack of reproducibility in the refractive index. This has been attributed to the hysteresis phenomenon typically present in reactive sputtering [14]. Therefore, the region around 200 W has been excluded from the following discussion.

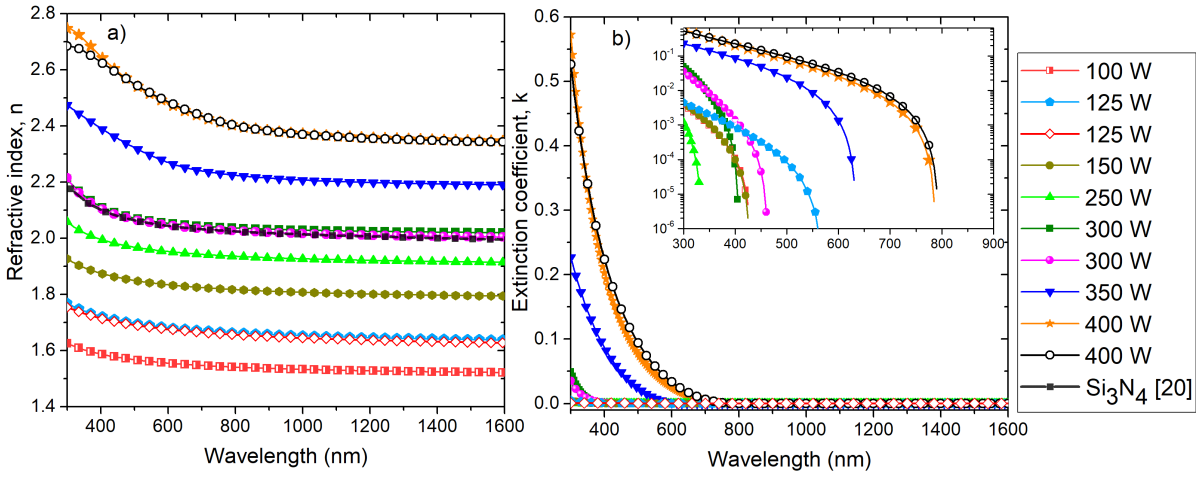

Figure 2: Refractive index (a) and extinction coefficient (b) trends for several samples produced at various sputtering powers. The inset shows the extinction coefficient in semi-logarithmic scale. The overlapped curves at 125 W, 300 W, and 400 W show the reliability of the experiment.

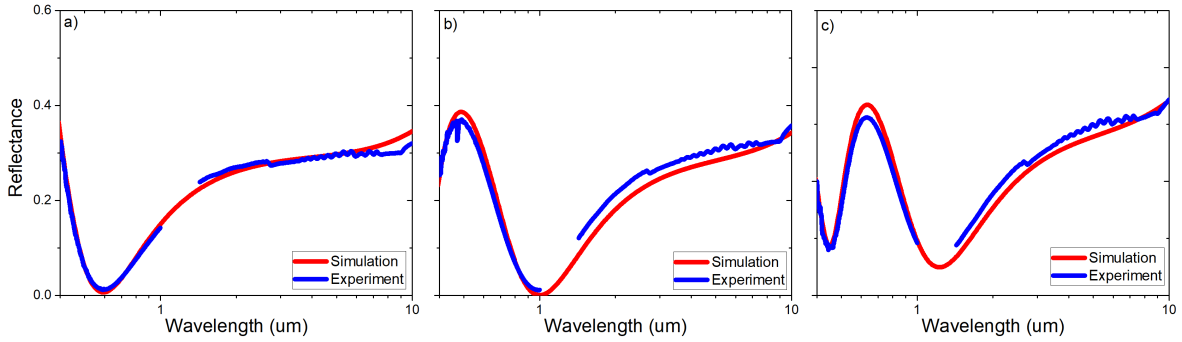

Figure 3: Reflectance measurements (blue lines) and simulations performed with Open Filters software (red line) on three samples at various sputtering power: 150 W (a), 300 W (b), and 400 W (c).

Fig. 2 shows the refractive indices and extinction coefficients trends in the range from 300 nm to 1600 nm, obtained from ellipsometric measurements on samples deposited at different powers. As it can be observed, the shape of the curves in Fig. 2 a) is similar for all the samples, while increasing the power results in an increased value for both the refractive index and the extinction coefficient, at each wavelength λ. This behavior could be qualitatively explained considering that the plasma confined nearby the target determines a release of silicon particles proportional to the RF power. Therefore, the increase in the RF power causes the consumption of nitrogen particles and the formation of silicon-rich SiN_x films. Hence, the samples deposited at powers higher than 300 W are characterized by refractive index values that overcome that of the stoichiometric Si_3N_4 reported in [20] (black squares in Fig. 2 a), which is almost perfectly matched by the film deposited at 300 W (olive green squares and magenta circles in Fig. 2 a). Films deposited at powers lower than 300 W are instead described by lower refractive indices: due to the low atomic ratio (Si/N) values, the ionized nitrogen can be easily backscattered from the cathode and be trapped into the growing film. This introduces lattice defects and distances the SiN_x films from the stoichiometric one. A similar behavior has been observed in the past [21]. As for the extinction coefficient in Fig. 2 b), it assumes values lower than 0.05 for powers up to 300 W, dropping rapidly to zero before reaching wavelengths of 600 nm; while for sputtering powers higher than 300 W it is no longer negligible and it drops to zero only at $\lambda > 600$ nm. The Tauc-Lorentz dispersion model also returns the band gap energy values, which are equal to 295 nm, 395 nm, 498 nm, and 579 nm for the film deposited at 250 W, 300 W, 350 W, and 400 W, respectively. Therefore, we can conclude that all samples results completely transparent in the near-IR region and most of them are nearly transparent also in the visible region.
Finally, the overlapped curves at 125 W (light blue pentagon and empty red rhombuses), 300 W (magenta circles and olive green squares) and 400 W (orange stars and empty black circles) in Fig. 2 a) and b) show that the reproducibility in deposition rate showed in Fig. 1 corresponds to a reproducibility of the refractive index curves, with a variation lower than 1%.

Reflectance study: integrating sphere and FTIR

The reflectance of three different samples taken as a reference are depicted in Fig. 3. The experimental results (blue lines) are compared with the simulation (red line), showing a very good agreement in the whole range of investigated wavelengths. To cover the broad spectral range from visible to IR, two different characterization techniques are used: for wavelengths from 0.3 μm to 1.75 μm, the reflectance has been measured using the integrating sphere; for wavelengths above 1.4 μm, FTIR measurements have been carried out. The region between 1 μm and 1.4 μm has been purposely avoided in the figure, since the transparency of the Si substrate above 1.1 μm alters the measurement. Simulations have been performed by using the experimental refractive index data presented in the section 3.1, which have been extended outside the measured wavelength range using the model data.
Fig. 4 shows the IR reflectance spectra of the three aforementioned silicon nitride films deposited at different

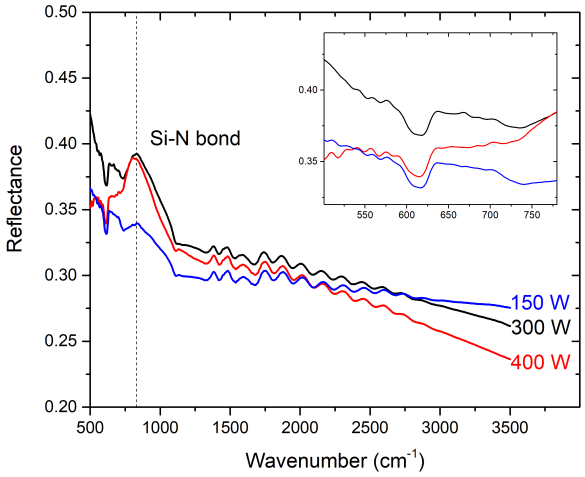

Figure 4: IR reflectance spectra of silicon nitride films deposited 150 W (blue line), 300 W (black line), and 400 W (red line) RF power. Inset: focus on the medium frequency region, from 500 to 750 cm^{-1}.

sputtering powers. For all the samples is evident a strong absorption band around 830 cm^{-1}, corresponding to the stretching vibration mode of the Si-N bond.The vibrations in the medium frequency range, i.e. 500 to 750 cm^{-1}, can be ascribed to vibrations of Si atoms in Si-N_4 tetrahedra [22]. The absence of additional peaks in the spectra suggests the absence of oxygen and hydrogen atoms in the chamber during the depositions, which otherwise could have participated in the formation of N-H, Si-H, N-H2 bending or stretching modes, as mostly happens in CVD depositions [23].

SEM analysis

The SEM analysis shows defect-free, homogeneous and featureless surface for each of the investigated sample. Fig. 5 show a map of SEM images of three silicon nitride films deposited at various sputtering powers. Each row refers to different powers, from 150 W (a-c) to 400 W (g-i), whereas columns refers to different magnification factors, M, from 1 to 10 KX, step 5 KX.

AFM analysis

The AFM analysis carried out with a XE-70 Park System on silicon nitride films deposited at different powers shows quite flat samples, with roughness average values below 1 nm. The analysis points out that the surface roughness decreases with increasing the sputtering power, according to results obtained in previous work [24]. Fig. 6 illustrates the 3D images of the samples over a sampling area of 500 nm x 500 nm: the roughness average values, R_a, ranges from 0.51 nm (at 150 W) to 0.30 nm (at 400 W), while the root mean square roughness (RMS) varies in 0.71 nm (at 150 W) to 0.43 nm (at 400 W). Both quantities have been evaluated by means of Gwyddion [25], a free and open source software for scanning probe microscopy data visualization and analysis.

4. Conclusions

SiN_x thin films have been deposited by RF magnetron sputtering at room temperature at fixed Ar and N_2 partial pressures and variable sputtering powers in the range of 100 to 400 W. Silicon nitride films with stoichiometric (Si_3N_4) optical properties have been obtained for an RF power of 300 W and a N_2 flow of 3 sccm. The increasing of the sputtering power results in the increase of the deposition rate and of both the refractive index and the extinction coefficient. This behavior has been clarified by considering the role of the sputtering power in the formation of the plasma, and in the ionization reactions.

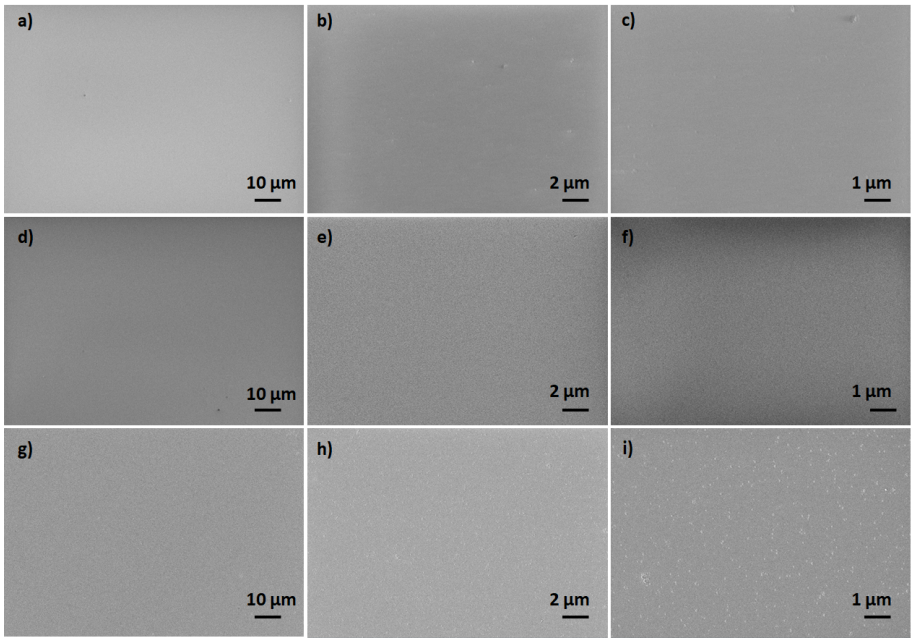

Figure 5: SEM micrographs map of SiN_x films deposited at 150 W (top row), 300 W (middle row), and 400 W (bottom row), with increasing magnitude: 1 KX (left column), 5 KX (middle column), 10 KX (right column).

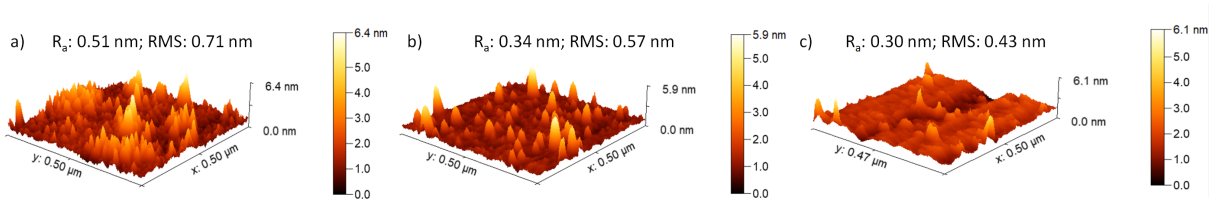

Figure 6: Atomic force micrographs of SiN_x films: 3D images over a 500x500 nm^2 region for the samples deposited at a sputtering power of 150 W (a), 300 W (b), and 400 W (c).

Reflectance measurements showed a good agreement with simulations in the whole range of investigation, also highlighting the presence of a Si-N bond and of Si vibrations in the IR region. Scanning electron microscope images and the atomic force microscope analysis show defect-free and homogeneous surfaces, suitable for the production of optical coatings.
The presented methodology proposes a method to control the refractive index in optical multilayer structures simply by adjusting the RF discharge power in a sputtering system equipped with a single cathode of Si. In sputtering systems with more than one cathode, the proposed method can be useful to increase the number of layers with different refractive index beyond the number of available targets, making it easier to achieve the desired optical response. Finally, we remark that the range of refractive index values could be further extended by lowering the refractive indices with the addition of oxygen as a process gas, to form SiO_xN_y or SiO_2.

Acknowledgments

The Ph.D. grant of two of the authors (DDL, AC) is funded by the PON2014-2020 "Dottorati innovativi con caratterizzazione industriale, XXXIV ciclo" program. The Ph.D. grant of one of the authors (DDM) is funded by the CNR-Confindustria "Dottorati di Ricerca Industriali" program XXXIV ciclo.
We thank Prof. Peter Bermel and David Kortge for valuable discussions.

References

[1] A. E. Kaloyeros, Y. Pan, J. Goff, B. Arkles, Review - silicon nitride and silicon nitride-rich thin film technologies: State-of-the-art processing technologies, properties, and applications, ECS Journal of Solid State Science and Technology 9 063006 (2020). doi:10.1149/2162-8777/aba447.

[2] C. E. Morosanu, The preparation, characterization and applications of silicon nitride thin films, Thin Solid Films 65 (1980) 171–208. doi:10.1016/0040-6090(80)90254-0.

[3] Z. Krstic, V. D. Krstic, Silicon nitride: the engineering material of the future, J. Mat. Sci. 47 (2012) 535–552. doi:10.1007/s10853-011-5942-5.

[4] M. D. Dange, J. Lee, K. Sooriakumar, New applications of low temperature PECVD silicon nitride films for microelectronic device fabrication, Microelec. J. 22 (1991) 19–26. doi:10.1016/0026-2692(91)90010-K.

[5] Q. Wilmart, H. El Dirani, N. Tyler, D. Fowler, S. Malhouitre, S. Garcia, M. Casale, et al., A versatile silicon-silicon nitride photonics platform for enhanced functionalities and applications, Appl. Sci. 9(2) (2019) 255. doi:10.3390/app9020255.

[6] M. Lipinski, Silicon nitride for photovoltaic application, Arc. Mat. Sc. Eng. 46(2) (2010) 69–87.

[7] C. Savall, J. Bruyère, J. Stoquert, Chemical bonds and microstructure in nearly stoichiometric PECVD $a\mathrm{Si}_x\mathrm{N}_y\mathrm{H}_z$, Thin Solid Films 260 (1995) 174–180. doi:10.1016/0040-6090(94)06476-8.

[8] M. Vila, C. Prieto, J. Garcia-Lopez, M. A. Respaldiza, Influence of the target and working gas on the composition of silicon nitride thin films prepared by reactive RF-sputtering, Nucl. Instrum. Methods Phys. Res. B 211 (2003) 199–205. doi:10.1016/S0168-583X(03)01211-4.

[9] F. Gao, Q. Zhao, X. Zhao, Y. Dong, Influence of substrate temperature on silicon nitride films deposited by R.F. magnetron sputtering., Adv. Mat. Research 150–151 (2010) 1391–1395. doi:10.4028/www.scientific.net/AMR.150-151.1391.

[10] S. Guruvenket, J. Ghatak, P. V. Satyam, G. M. Rao, Characterization of bias magnetron-sputtered silicon nitride films, Thin Solid Films 478 (2005) 256–260. doi:10.1016/j.tsf.2004.10.031.

[11] M. A. Signore, A. Sytchkova, D. Dimaio, A. Cappello, A. Rizzo, Deposition of silicon nitride thin films by RF magnetron sputtering: a material and growth process study, Opt. Mat. 34 (2012) 632–638. doi:10.1016/j.optmat.2011.09.012.

[12] M. Vila, C. Prieto, P. Miranzo, M. I. Oscendi, R. Ramirez, Characterization of $\mathrm{Si}_3\mathrm{N}_4$ thin films prepared by r.f. magnetron sputtering, Surf. Coat. Tech. 151-152 (2002) 67–71. doi:10.1016/S0257-8972(01)01600-0.

[13] E. Sarhammar, K. Strijckmans, T. Nyberg, S. Van Steenberge, S. Berg, D. Depla, A study of the process pressure influence in reactive sputtering aiming at hysteresis elimination, Surf. Coat. Tech. 232 (2013) 357–361. doi:10.1016/j.surfcoat.2013.05.035.

[14] K. Strijckmans, R. Schelfhout, D. Depla, Tutorial: Hysteresis during the reactive magnetron sputtering process, J. App. Phys. 124) (2018) 241101–1, 241101–29. doi:10.1063/1.5042084.

[15] J. Y. Horiba, Tauc-lorentz dispersion formula, Tech. rep. (2006).

[16] G. E. Jellison, F. A. Modine, Parameterization of the optical functions of amorphous materials in the interband region, Appl. Phys. Lett. 69 (1996). doi:10.1063/1.118064.

[17] S. Larouche, L. Martinu, Open filters: open-source software for the design, optimization, and synthesis of optical filters, Appl. Opt. 47 (2008) C219–C230. doi:10.1364/AO.47.00C219.

[18] P. S. Nayar, Refractive index control of silicon nitride films prepared by radio-frequency reactive sputtering, J. Vac. Sci. Tech. A 20 (2002) 2137. doi:10.1116/1.1513637.

[19] M. K. Mustafa, U. Majeed, Y. Iqbal, Effect on silicon nitride thin films properties at various powers of rf magnetron sputtering, Int. J. Eng. Tech. 7 (2018) 39–41. doi:10.14419/ijet.v7i4.30.22000.

[20] K. Luke, Y. Okawachi, M. R. E. Lamont, A. L. Gaeta, M. Lipson, Broadband mid-infrared frequency comb generation in a $\mathrm{Si}_3\mathrm{N}_4$ microresonator, Opt. Lett. 40 (2015) 4823–4826. doi:10.1364/OL.40.004823.

[21] K. Matsuzaki, A. Hirabayashi, M. Saga, Characterization of reactively sputtered silicon nitride, J. Electrochem. Soc. 139 (1992).

[22] D. Legut, U. D. Wdowik, P. Kurtyka, Vibrational and dielectric properties of α-$\mathrm{Si}_3\mathrm{N}_4$ from density functional theory, Mat. Chem. Phys. 147 (1-2) (2014). doi:10.1016/j.matchemphys.2014.03.058.

[23] G. N. Parsons, J. H. Souk, J. Batey, Low hydrogen content stoichiometric silicon nitride films deposited by plasmaenhanced chemical vapor deposition, J. Appl. Phys. 70 (1991) 1553. doi:10.1063/1.349544.

[24] V. Bhatt, S. Chandra, Silicon nitride films deposited by rf sputtering for microstructure fabrication in MEMS, J. El. Mat. 38 (2009) 1979–1989. doi:10.1007/s11664-009-0846-8.

[25] gwyddion.net.